THE JOURNAL OF PHYSICAL CHEMISTRY A

pubs.acs.org/JPCA Article

Quantum Mechanical Modeling of Reaction Rate Acceleration in Microdroplets

Namita Narendra, Xingshuo Chen, Jinying Wang, James Charles, R. Graham Cooks,* and Tillmann Kubis*

Cite This: J. Phys. Chem. A 2020, 124, 4984–4989

Read Online

ACCESS | Metrics & More | Article Recommendations

ABSTRACT: Organic reactions in microdroplets can be orders of magnitude faster than their bulk counterparts. We hypothesize that solvation energy differences between bulk and interface play a key role in the intrinsic rate constant increase and test the hypothesis with explicit solvent calculations. We demonstrate for both the protonated phenylhydrazine reagent and the hydrazone transition state (TSB) that molecular orientations which place the charge sites at the surface confer high energy. A pathway in which this high-energy form transforms into a fully solvated TSB has a lower activation energy than bulk by some 59 kJ/mol, a result that is consistent with experimental rate acceleration studies.

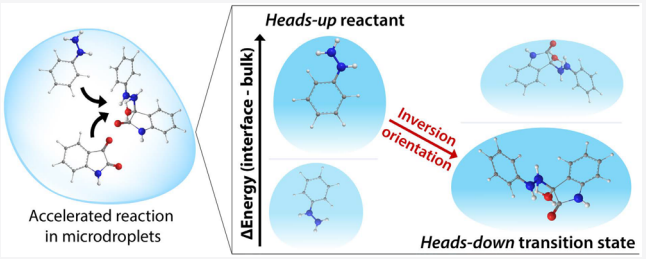

I. INTRODUCTION

Recent studies show that for a number of organic reactions the rate in the bulk solution phase is often much smaller than that in microdroplets.[1,2] This phenomenon, known as reaction rate acceleration, is associated with increased reaction rates near the surface, evidenced by the fact that acceleration increases strongly in smaller droplets with larger surface/volume ratios.[3,4] Droplets of interest have usually been formed by spray-based mass spectrometry (MS) ionization methods such as electrospray ionization (ESI),[5,6] desorption electrospray ionization (DESI),[7] paper spray (PS),[8] and field desorption (FD).[9] Alternatively, droplets have been generated by thermal[4,10] or electromagnetic levitation.[11,12] The typical diameters of the droplets generated by ESI are in the hundreds of nanometers range.[13] Rate acceleration has also been reported in other confined volume systems, such as thin films (2D variants of microdroplets)[10] as well as at interfaces between two phases.[14] The large magnitude of the rate accelerations reported for microdroplets (orders of magnitude in microdroplets) has aroused interest since they offer potential for the development of high-throughput methods of selecting optimum reaction conditions and synthesizing compounds on a small scale.[15]

The underlying reason for the large rate acceleration in microdroplets is being explored through a variety of experiments.[1−3] These show clearly that confined volume systems differ from their bulk counterpart in reaction rates which parallel the dramatically increased surface area/volume ratios. This implies that interfacial reactions play a key role in reaction acceleration. In particular circumstances, contributions to rate acceleration can be made by increased reagent concentration associated with solvent evaporation.[7,8] Most interesting are the intrinsic effects that increase rate constants. Among those suggested are the reduced collision times of reagents in small compartments,[16] the high electric field at the interface in the case of aqueous microdroplets,[17] and the decreased solvation energy of reagent molecules at the droplet (or thin film) interface.[1] This computational study explores the possibility that solvation energy differences at the interface and in the bulk are responsible for the increase in intrinsic rate constants. Unlike the situation in bulk solvents, where reagents must overcome large solvation barriers to form the activated complex, reagents near the interface may be less solvated and so have a lower activation energy.[1,16,18,19]

To explore the mechanism of reaction acceleration in droplets computationally, one needs a method that explicitly considers solvent molecules when calculating the energies and structures of the reagents and the transition state. Density functional tight binding (DFTB) methods are used to provide the energies of solution phase reagents and intermediates in the bulk and at various distances from the interface. Note that the computation does not consider entropic factors affecting reaction rate constants, just energies without any computation

Received: April 10, 2020
Revised: May 23, 2020
Published: May 26, 2020

https://dx.doi.org/10.1021/acs.jpca.0c03225
J. Phys. Chem. A 2020, 124, 4984–4989

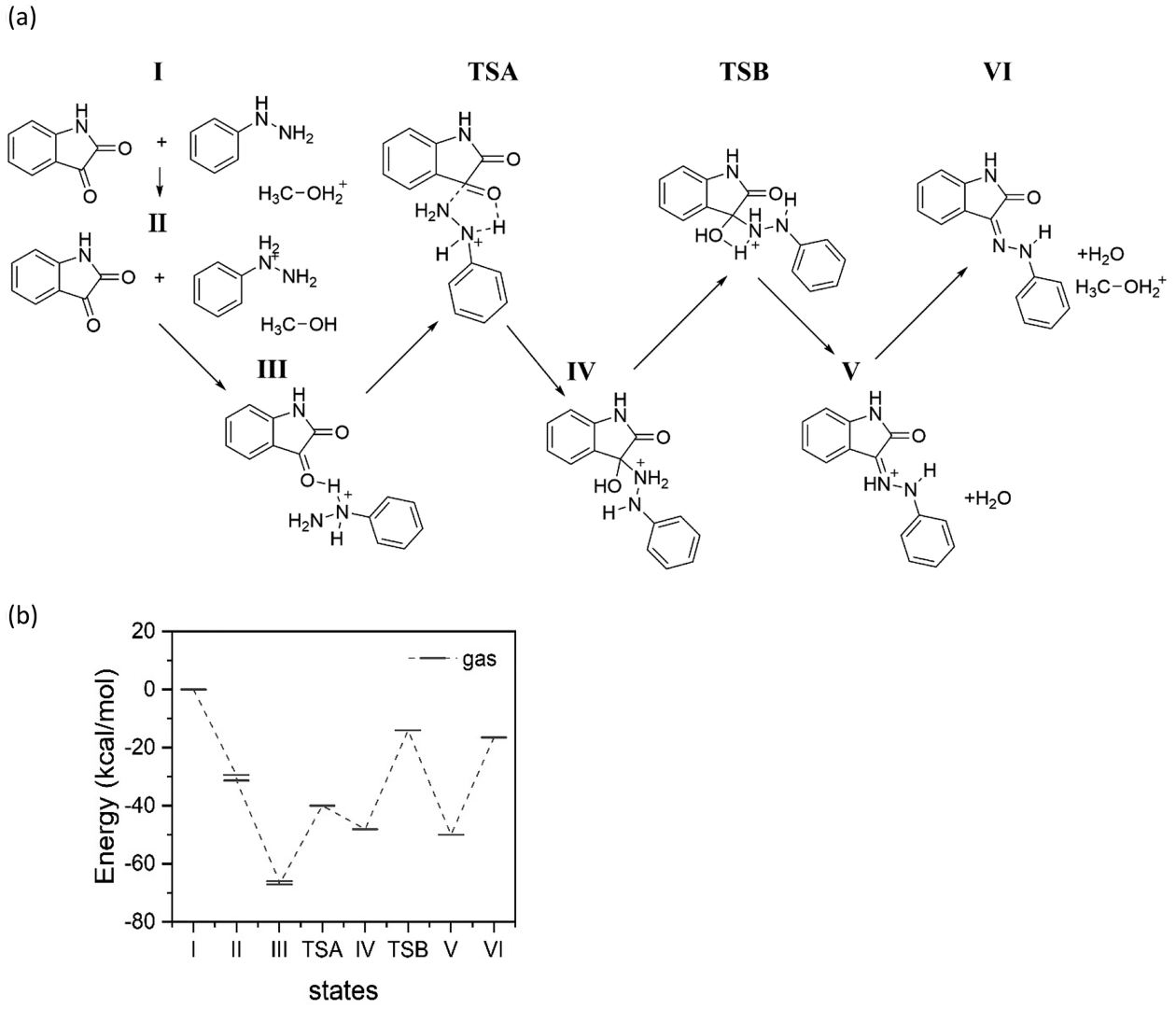

Figure 1. (a) Reaction pathway adapted from ref 25. (b) Energies of all the states along the reaction coordinate for hydrazone formation calculated (this work) by using B3LYP density functional theory and 6-31G(d,p) basis sets. Note the two conformations of structures II and III.

of reaction dynamics which would not be computationally possible at the scale used here.

The particular chemical reaction chosen for modeling is hydrazone formation by reaction of phenylhydrazine and indoline-2,3-dione in HCl/methanol. This reaction has been reported to be accelerated by a factor of 10^4 when the initially generated nESI droplets are allowed to undergo extensive evaporation.[20] The degree to which the rate constant is increased by this concentration effect is not known. In this study we use ab initio computations to estimate the activation energy at the surface and in the bulk to elucidate the cause of the rate acceleration in microdroplets.

II. METHODS

Gaussian[21] is used to determine the reaction pathway in the gas phase. It is assumed that the pathway is not affected by the methanol solvent or interfacial nature of the reaction. Geometry optimization is performed by using B3LYP density functional theory[22] and 6-31G(d,p) basis sets.

Once the geometry of the reaction intermediates is determined, the next step is to determine the energetics of reagents and transition state at the droplet surface. Interface calculations require explicit solvent simulation with thousands of atoms. Gaussian or standard DFT approaches are not computationally feasible. Self-consistent density functional tight binding (SCC-DFTB) allows quantum mechanical calculations at a large scale. SCC-DFTB as implemented by the package DFTB+ is used; it is based on a second-order expansion of the Kohn−Sham total energy with respect to the charge density fluctuations.[23]

$$E_{\text{total}}^{\text{SCC-DFTB}} = \sum_{i\mu\nu} c_\mu^i c_\nu^i H_{\mu\nu}^0 + \frac{1}{2}\sum_{\alpha\beta}\gamma_{\alpha\beta}\Delta q_\alpha \Delta q_\beta + E_{\text{rep}}$$

Here $H_{\mu\nu}^0$ is the Hamiltonian matrix elements, c_μ^i and c_ν^i are the wave function coefficients, Δq_α and Δq_β are the Mulliken net charges induced on orbitals α and β interacting through the Coulomb potential $\gamma_{\alpha\beta}$, and E_{rep} is the short-range repulsion term. Note that the total energy does not have any contribution from the entropy. The Slater−Koster parameter set used is 3ob-3-1 which is optimized for biomolecules and organic molecules.[24]

An estimation of the reaction rate increase at the interface requires calculation of the activation energy both in bulk methanol and at the methanol−vacuum interface, where

https://dx.doi.org/10.1021/acs.jpca.0c03225
J. Phys. Chem. A 2020, 124, 4984−4989

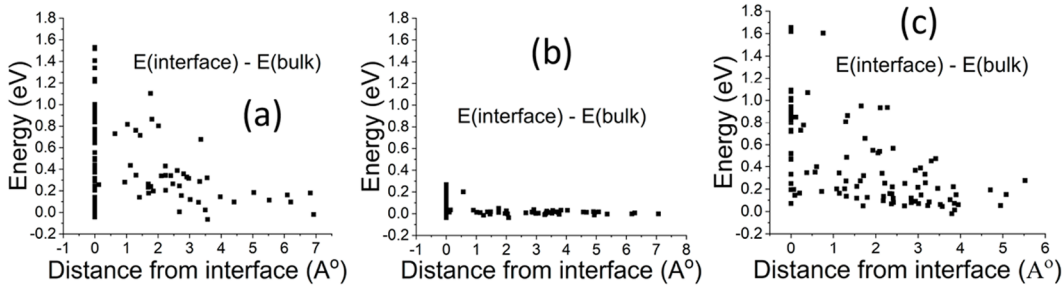

Figure 2. Difference in energy between interface and bulk plotted as a function of distance from the interface for target molecules in methanol. One hundred configurations were randomly chosen with the target molecule at the distances shown for (a) protonated phenylhydrazine, (b) indoline-2,3-dione, and (c) TSB.

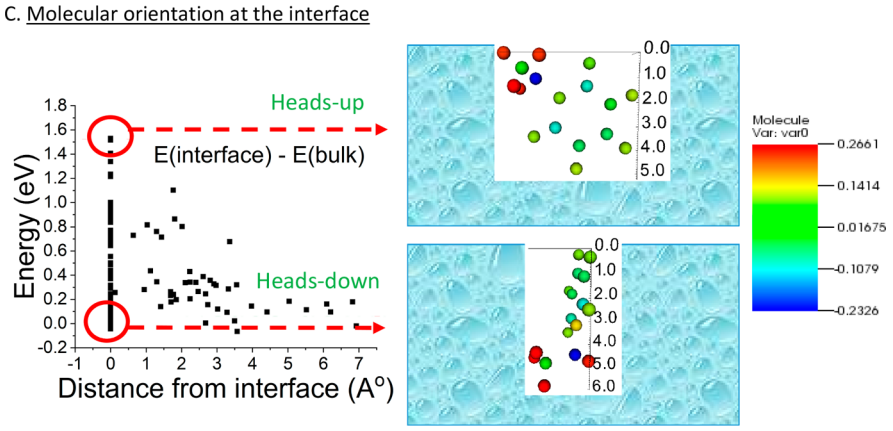

Figure 3. (left) Charge distribution analysis for protonated phenylhydrazine at the interface revealing two categories: heads-up and heads-down. A selected pair of structures is visualized. The *z*-coordinates are indicated next to the molecular structure in units of Å. The color scale at right represents the charge of the atoms in units of the electron charge. Red indicates high positive charge while blue indicates high negative charge. The three hydrogens on the terminal N carry the most positive charge and the adjacent N the most negative charge.

vacuum substitutes for the air of the experiment. This involves simulation of three separate molecules in the solvent—the two reactants and the transition state. They are termed target molecules henceforth. The target molecules are considered individually in the solvent, one at a time. The effect of target molecule interaction with each other on the activation energy is not considered as this is regarded as a second-order effect. For the bulk calculation, a cubic solvent box of dimension 2.5 nm is used with periodic boundary conditions. The 2.5 nm distance is sufficient to minimize the interaction of the target molecule with its periodic target molecule neighbors.

The solvent box is filled with methanol molecules by using PACKMOL.[25] The initial configuration is generated by packing with density of 0.791 g/mL and inserting one target molecule. Structural optimization is performed with SCC-DFTB until the force on the atoms is $<10^{-4}$ eV/Å using the LBFGS algorithm. All the simulations are performed with Γ point sampling of the solvent box. To create the interfacial structure, the bulk methanol solvent box is sliced in the *XY* plane at or just above (over the range 0−7 Å) the point where the target molecule is present and a vacuum of 1.5 nm is added. This process is repeated to create 100 such correlated bulk and interface structures for each target molecule starting from the random PACKMOL configurations. Note that this procedure correlates bulk and interface structures and so helps isolate the effects of the interface. Once the interface structure is created, there is no further structural optimization in SCC-DFTB. Electronic relaxation with SCC-DFTB provides atom resolved energies which allows for calculation of target molecule energy in bulk and in the interfacial region.

III. RESULTS AND DISCUSSION

A. Reaction Pathway. Acid-catalyzed hydrazone formation from phenylhydrazine and indoline-2,3-dione in microdroplets was selected to investigate the activation energy difference between reactions at the interface and in the bulk. The proposed reaction pathway, shown in Figure 1, is taken to be that of the gas phase reaction of hydrazine itself with simple carbonyl compounds as studied by flowing afterglow.[26] This is a complex process with many states potentially involved, and a mechanism like that in Figure 1 has been proposed for the aqueous phase reaction.[27] Transition state TSA corresponds to formation of a C−N bond through nucleophilic attack by the phenylhydrazine while TSB corresponds to loss of water; these states are exactly analogous to those suggested by Bierbaum and co-workers.[26] Calculations show that formation of TSB has the highest energy barrier along the potential energy surface in the gas phase reaction pathway and is thus the rate-limiting step. The energy difference between the reactants and TSB is used to estimate the activation energy in the following discussion. Alternative pathways are possible but are not explored in this paper because of the large computational effort involved and the fact that the key features of solvation-mediated energies are likely to occur in any related mechanism.

B. Energetics at the Interface. We hypothesize that solvation plays an important role in decreasing the activation

https://dx.doi.org/10.1021/acs.jpca.0c03225
J. Phys. Chem. A 2020, 124, 4984−4989

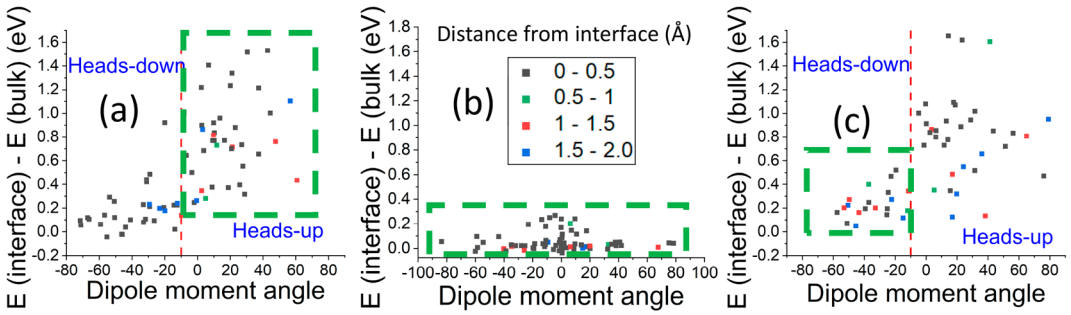

Figure 4. Plot of difference in energy between interface and bulk for target molecules as a function of dipole moment angle with respect to the interface for (a) protonated phenylhydrazine, (b) indoline-2,3-dione, and (c) TSB. The green dashed rectangle shows the data points selected for averaging in the activation energy calculation. The color coding shows the distance from the interface and applies to all three parts of the figure.

energy and that this effect is smaller at the interface than in the bulk. To investigate this, we prepared by methods described in the Methods section a set of random configurations of the target molecules in methanol where the distance of the target molecule from the interface is systematically varied. The effect of solvation on the energy of the reagents (indoline-2,3-dione and protonated phenylhydrazine) and the rate-limiting intermediate, TSB, was examined by performing 100 simulations of each of these target molecules. This solvent explicit energy calculation was performed by using SCC-DFTB at various distances from the methanol/vacuum interface. The results are plotted in Figure 2 as the energy difference between the bulk and interface as a function of distance from the interface.

It can be seen that both protonated phenylhydrazine and TSB exhibit a large spread in energy for individual randomly selected orientations at and near the interface. The energy of protonated phenylhydrazine and TSB molecules at the interface can increase by as much as 1.53 and 1.65 eV, respectively, relative to bulk; this can be explained by the degree of solvent stabilization of the positive charge site of the molecule. This interfacial effect vanishes some 4 Å from the interface. On the other hand, the energy difference for the uncharged indoline-2,3-dione molecule is much smaller, and it vanishes above 1 Å.

C. Molecular Orientation at the Interface. To gain a better understanding of the large distribution of energies at the interface, the molecular orientation and charge distribution of representative protonated phenylhydrazine molecules with different energies are visualized in Figure 3. (The tendency for ions to be located near the interface of droplets is an established assumption in studies of accelerated reactions in microdroplets.[28]) The most energetic molecules at the interface are found to correspond to "heads-up" configurations, namely those with the positive charge center at or near the interface. Heads-up configurations of the reactants are least solvated by methanol and thus represent the most reactive configurations. Therefore, we hypothesize that the greatly enhanced reaction rate in microdroplets is attributed reaction sequences that start from "heads-up" configurations. By contrast, the least energetic molecules correspond to "heads-down" configurations whose positive charge centers are far from the surface. These "heads-down" configurations, with their charge centers solvated by methanol, resemble bulk-phase target molecules and are of less interest. Similar observations were made for the charged TSB molecules. There is a wide energy distribution among molecules due to different orientations of positive charge center, with the "heads-up" configurations as the most energetic form and "heads-down" configurations as the less energetic forms. If the formation of TSB from the heads-up reactants is accompanied by rotation, the forming reaction complex energy will be released to form the most stable configuration, i.e., the heads-down configuration. So we further conclude that heads-up reagent ions correlating with heads-down TSB represents the energetically most favorable pathway.

To systematically classify target molecule configurations as heads-up or heads-down, the angle of the dipole moment of the target molecule with respect to the plane of the interface is considered, as shown in Figure 4. Both charged target molecules show a strong correlation of high energy/positive dipole vs low energy/negative dipole. Configurations with zero dipole moment angle lie in the plane of the interface; configurations with positive dipole moment angle are classified as heads up-configurations while those more negative are classified as heads-down. This clearly establishes a high-energy/heads-up relationship for the charged target molecules while the uncharged indoline-2,3-dione show no such configurational preference.

D. Rate Acceleration Calculation. To assess the rate acceleration between interface and bulk, we need to derive reaction rates from the activation energy. The reaction rate R is proportional to the reaction rate constant k, where $k \propto e^{-E_a/k_B T}$ (k_B is the Boltzmann constant, T is the temperature, and E_a is the activation energy given by $E_a = E_{\text{transition state}} - \sum E_{\text{reactants}}$). The reaction rate acceleration at the interface is given by the ratio of rate constants $k_{\text{interface}}/k_{\text{bulk}}$ which is equal to $g[e^{-(E_{a,\text{interface}} - E_{a,\text{bulk}})/k_B T}]$. Here, g is the ratio of pre-exponential factors of the rate constants for the interface and bulk.

The reaction acceleration at the interface is dominated by the least solvated and hence most reactive "heads-up" configurations of protonated phenylhydrazine molecules at the interface. If we assume that there is no change in the molecule configuration along the reaction pathway from the reactant molecules to TSB, then there will be no rate acceleration at the interface. But experiments show that reaction acceleration is observed in microdroplets. From this, it follows that the change in configuration along the reaction pathway is at least an explanation of reaction acceleration at the interface. The upper limit of the rate acceleration is when there is a full change in the configuration from "heads-up" protonated phenylhydrazine to "heads-down" TSB.

To explore this point and gain further insight, the energies of the "heads-up" ("heads-down") configurations of protonated

https://dx.doi.org/10.1021/acs.jpca.0c03225
J. Phys. Chem. A 2020, 124, 4984−4989

phenylhydrazine (TSB) lying within 0−1 Å of the interface were averaged. In the case of the uncharged indoline-2,3-dione, all the configurations within the 0−1 Å range were considered given that there is only a slight effect of orientation on energy.

By averaging over the selected configurations (within the green dashed boxes in Figure 4) and considering only those target molecules within the 1 Å distance from the interface, the average difference in energy between interface and bulk for the target molecules is tabulated in Table 1. This results in a 612

Table 1. Difference in Average Energies at Interface and Bulk for Reagents Involved in Hydrazone Formation

target molecule	protonated phenylhydrazine	indoline-2,3-dione	TSB
E(interface) − E(bulk) (eV)	0.821	0.056	0.265

meV decrease in activation energy from bulk to interface. Ignoring the pre-exponential g-factor, this corresponds to an upper bound in reaction rate acceleration of 1.89×10^{10} at the methanol/vacuum interface at 300 K.

E. Discussion on Methodology. Some aspects of the methodology should now be discussed and will be examined in more detail in the future. They include the following:

(i) The use of solvent correlation between bulk and interfacial target molecules. This was necessary to constrain the computational time required to cover all the possible structural phase space to a practicable limit (even so, the total computation time for the results shown in this study was approximately 60000 core hours). Solvent correlation helps minimize the noise arising from the difference in the solvent molecule orientations surrounding the target molecule between bulk and interface. The process helps to isolate the impact of the interface on the target molecule energy from other factors.

(ii) The effect of relaxation of the solvent at the interface was not considered. Preliminary calculations show that such interface relaxation reduces the average difference in energy between interface and bulk by nearly half compared to unrelaxed interface. Because the solvent configuration around the target molecules will change after interface relaxation, it is no longer accurate to compare the interface and bulk target molecule energies on a one-to-one basis. The qualitative analysis described above still holds after interface relaxation.

(iii) From equilibrium statistics, the likelihood of "heads-up" protonated phenylhydrazine to occur is very low ($\sim 10^{-6}$). This probability is obtained by the density matrix approach. The statistical weight of each sample is given by $e^{-E_n/k_BT}/Z$, where Z is the partition function $\sum_n e^{-E_n/k_BT}$. If one corrects for this probability, the upper bound of the rate acceleration is 10^4. The bulk rate constant is not known accurately for methanol, but a similar case[29] reports a value of ca. 10 M^{-1} s^{-1} which, when considered with the Bain et al. acceleration factor of 10^4, gives an approximate interfacial value of 10^5 M^{-1} s^{-1} or, converting units, 2×10^{-16} cm^3 $molecules^{-1}$ s^{-1}. The gas phase reaction rate is $\sim 10^{-9}$ cm^3 $molecules^{-1}$ s^{-1}, which is still orders of magnitude faster than the accelerated interfacial reaction.

We note also that acceleration at the microdroplet surface due to "heads-down" protonated phenylhydrazine is negligible. This leads us to wonder whether the dynamics of evaporation can increase the nonequilibrium probability of occurrence of "heads-up" configurations. Molecular dynamics would be needed to capture all features of the reaction trajectory and the entropy information which is beyond the scope of the current paper. We note that prior validation tests used only static SCC-DFTB with geometry relaxation and thermodynamic integration methods to calculate the solvation energy of a single molecule in an explicit liquid.[25] Because our results were comparable with literature, this increases confidence in the applicability of static SCC-DFTB to the current application.

IV. CONCLUSION

Explicit solvent calculation of energies shows that protonated phenylhydrazine, when oriented with the charge site at or near the surface, is a partly solvated high-energy species. Reagent ions with the opposite orientation have energies that approach values of the bulk species. It is proposed that a reaction pathway that would result in strong acceleration involves the reorientation of a "heads-up" phenylhydrazine to a "heads-down" TSB. The estimated upper bound value for the rate acceleration for hydrazone formation in microdroplets is about 10^{10}, but this factor is offset by the low statistical probability (ca. 1 in 10^6) of the heads-up configuration. The net result is consistent with the modest rate acceleration factor (one to a few orders of magnitude) seen in the experiment.[20] Some aspects of the methodology should be examined in more detail in the future. They include the use of solvent correlation between bulk and interfacial target molecules and the degree of solvent relaxation allowed. The main problem encountered in this study is that the questions raised can only be answered by a full treatment of reaction dynamics. Because nothing approaching this is possible, we have chosen to explore an extreme reaction trajectory (heads-up reagent at interface to heads-down transition state, with no other relaxation) and to evaluate its consequences. The results are encouraging in terms of the support they offer for the feasibility of the partial solvation hypothesis which, on the other hand, they do not prove.

AUTHOR INFORMATION

Corresponding Authors

R. Graham Cooks − *Department of Chemistry, Purdue University, West Lafayette, Indiana 47906, United States;* orcid.org/0000-0002-9581-9603; Email: cooks@purdue.edu

Tillmann Kubis − *Network for Computational Nanotechnology, School of Electrical and Computer Engineering, Center for Predictive Materials and Devices, and Purdue Institute of Inflammation, Immunology and Infectious Disease, Purdue University, West Lafayette, Indiana 47906, United States;* Email: tkubis@purdue.edu

Authors

Namita Narendra − *Network for Computational Nanotechnology, Purdue University, West Lafayette, Indiana 47906, United States*

Xingshuo Chen − *Department of Chemistry, Purdue University, West Lafayette, Indiana 47906, United States*

https://dx.doi.org/10.1021/acs.jpca.0c03225
J. Phys. Chem. A 2020, 124, 4984−4989

Jinying Wang − *Network for Computational Nanotechnology, Purdue University, West Lafayette, Indiana 47906, United States*

James Charles − *School of Electrical and Computer Engineering, Purdue University, West Lafayette, Indiana 47906, United States;* orcid.org/0000-0002-4212-7435

Complete contact information is available at: https://pubs.acs.org/10.1021/acs.jpca.0c03225

Notes

The authors declare no competing financial interest.

■ ACKNOWLEDGMENTS

We acknowledge support by the National Science Foundation (1905087).

■ REFERENCES

(1) Yan, X.; Bain, R. M.; Cooks, R. G. Organic Reactions in Microdroplets: Reaction Acceleration Revealed by Mass Spectrometry. *Angew. Chem., Int. Ed.* **2016**, *55*, 12960−12972.

(2) Banerjee, S.; Gnanamani, E.; Yan, X.; Zare, R. N. Can All Bulk-Phase Reactions Be Accelerated in Microdroplets? *Analyst* **2017**, *142*, 1399−1402.

(3) Zhou, Z.; Yan, X.; Lai, Y.-H.; Zare, R. N. Fluorescence Polarization Anisotropy in Microdroplets. *J. Phys. Chem. Lett.* **2018**, *9*, 2928−2932.

(4) Bain, R. M.; Pulliam, C. J.; Thery, F.; Cooks, R. G. Accelerated Chemical Reactions and Organic Synthesis in Leidenfrost Droplets. *Angew. Chem., Int. Ed.* **2016**, *55*, 10478−10482.

(5) Müller, T.; Badu-Tawiah, A.; Cooks, R. G. Accelerated Carbon−Carbon Bond-Forming Reactions in Preparative Electrospray. *Angew. Chem., Int. Ed.* **2012**, *51*, 11832−11835.

(6) Banerjee, S.; Zare, R. N. Syntheses of Isoquinoline and Substituted Quinolines in Charged Microdroplets. *Angew. Chem., Int. Ed.* **2015**, *54*, 14795−14799.

(7) Girod, M.; Moyano, E.; Campbell, D. I.; Cooks, R. G. Accelerated Bimolecular Reactions in Microdroplets Studied by Desorption Electrospray Ionization Mass Spectrometry. *Chem. Sci.* **2011**, *2*, 501−510.

(8) Yan, X.; Augusti, R.; Li, X.; Cooks, R. G. Chemical Reactivity Assessment Using Reactive Paper Spray Ionization Mass Spectrometry: The Katritzky Reaction. *ChemPlusChem.* **2013**, *78*, 1142−1148.

(9) Chen, X.; Cooks, R. G. Accelerated Reactions in Field Desorption Mass Spectrometry. *J. Mass Spectrom.* **2018**, *53*, 942−946.

(10) Wei, Z.; Wleklinski, M.; Ferreira, C.; Cooks, R. G. Reaction Acceleration in Thin Films with Continuous Product Deposition for Organic Synthesis. *Angew. Chem., Int. Ed.* **2017**, *56*, 9386−9390.

(11) Jacobs, M. I.; Davies, J. F.; Lee, L.; Davis, R. D.; Houle, F.; Wilson, K. R. Exploring Chemistry in Microcompartments Using Guided Droplet Collisions in a Branched Quadrupole Trap Coupled to a Single Droplet, Paper Spray Mass Spectrometer. *Anal. Chem.* **2017**, *89*, 12511−12519.

(12) Grimm, R. L.; Beauchamp, J. L. Field-Induced Droplet Ionization Mass Spectrometry. *J. Phys. Chem. B* **2003**, *107*, 14161−14163.

(13) Xia, Z.; Williams, E. R. Effect of Droplet Lifetime on Where Ions Are Formed in Electrospray Ionization. *Analyst* **2019**, *144*, 237−248.

(14) Yan, X.; Cheng, H.; Zare, R. N. Two-Phase Reactions in Microdroplets without the Use of Phase-Transfer Catalysts. *Angew. Chem., Int. Ed.* **2017**, *56*, 3562−3565.

(15) Wleklinski, M.; Loren, B. P.; Ferreira, C. R.; Jaman, Z.; Avramova, L.; Sobreira, T. J. P.; Thompson, D. H.; Cooks, R. G. High Throughput Reaction Screening Using Desorption Electrospray Ionization Mass Spectrometry. *Chem. Sci.* **2018**, *9*, 1647−1653.

(16) Mondal, S.; Acharya, S.; Biswas, R.; Bagchi, B.; Zare, R. N. Enhancement of Reaction Rate in Small-Sized Droplets: A Combined Analytical and Simulation Study. *J. Chem. Phys.* **2018**, *148*, 244704.

(17) Kathmann, S. M.; Kuo, I. F. W.; Mundy, C. J. Electronic Effects on the Surface Potential at the Vapor-Liquid Interface of Water. *J. Am. Chem. Soc.* **2008**, *130*, 16556−16561.

(18) Mortensen, D. N.; Williams, E. R. Ultrafast (1 Ms) Mixing and Fast Protein Folding in Nanodrops Monitored by Mass Spectrometry. *J. Am. Chem. Soc.* **2016**, *138*, 3453−3460.

(19) Hagberg, D.; Brdarski, S.; Karlström, G. On the Solvation of Ions in Small Water Droplets. *J. Phys. Chem. B* **2005**, *109*, 4111−4117.

(20) Bain, R. M.; Pulliam, C. J.; Ayrton, S. T.; Bain, K.; Cooks, R. G. Accelerated Hydrazone Formation in Charged Microdroplets. *Rapid Commun. Mass Spectrom.* **2016**, *30*, 1875−1878.

(21) Frisch, M. J.; Trucks, G. W.; Schlegel, H. B.; Scuseria, G. E.; Robb, M. A.; Cheeseman, J. R.; Scalmani, G.; Barone, V.; Petersson, G. A.; et al. *Gaussian 16*, Rev. A.03.; Gaussian, Inc.: Wallingford, CT, 2016.

(22) Stephens, P. J.; Devlin, F. J.; Chabalowski, C. F.; Frisch, M. J. Ab Initio Calculation of Vibrational Absorption and Circular Dichroism Spectra Using Density Functional Force Fields. *J. Phys. Chem.* **1994**, *98*, 11623−11627.

(23) Aradi, B.; Hourahine, B.; Frauenheim, T. DFTB+, a Sparse Matrix-Based Implementation of the DFTB Method †. *J. Phys. Chem. A* **2007**, *111*, 5678−5684.

(24) Gaus, M.; Goez, A.; Elstner, M. Parametrization and Benchmark of DFTB3 for Organic Molecules. *J. Chem. Theory Comput.* **2013**, *9*, 338−354.

(25) Allouche, A. Software News and Updates Gabedit — A Graphical User Interface for Computational Chemistry Softwares. *J. Comput. Chem.* **2011**, *32*, 174−182.

(26) Custer, T. G.; Kato, S.; Bierbaum, V. M.; Howard, C. J.; Morrison, G. C. Gas-Phase Kinetics and Mechanism of the Reactions of Protonated Hydrazine with Carbonyl Compounds. Gas-Phase Hydrazone Formation: Kinetics and Mechanism. *J. Am. Chem. Soc.* **2004**, *126*, 2744−2754.

(27) Sollenberger, P. Y.; Martin, R. B. In *The Chemistry of the Amino Group*; Patai, S., Ed.; Interscience Publ: London, 1968; Vol. *1*, pp 349−407.

(28) Wei, Z.; Li, Y.; Cooks, R. G.; Yan, X. Accelerated Reaction Kinetics in Microdroplets: Overview and Recent Developments. *Annu. Rev. Phys. Chem.* **2020**, *71*, 31−51.

(29) Kool, E. T.; Park, D. H.; Crisalli, P. Fast Hydrazone Reactants: Electronic and Acid/Base Effects Strongly Influence Rate at Biological PH. *J. Am. Chem. Soc.* **2013**, *135*, 17663−17666.